

Journal of Organometallic Chemistry, 410 (1991) 389–401
 Elsevier Sequoia S.A., Lausanne
 JOM 21806

Synthesis and structural characterisation of tris(diphenylthiophosphinoyl)methane and tris(diphenylthiophosphinoyl)methanide complexes of rhodium and iridium; X-ray structures of $[\text{Rh}(\text{C}_8\text{H}_{12})\{\eta^2\text{-C}(\text{P}(\text{S})\text{Ph}_2)_3\text{-S,S}\}]$ and $[\text{Ir}(\text{CO})_2\{\eta^2\text{-C}(\text{P}(\text{S})\text{Ph}_2)_3\text{-S,S}\}]$

Jane Browning, Keith R. Dixon ^{*}, Robert W. Hiltz, Neil J. Meanwell
 and Fang Wang

Department of Chemistry, University of Victoria, Victoria, British Columbia V8W 3P6 (Canada)
 (Received November 28th, 1990)

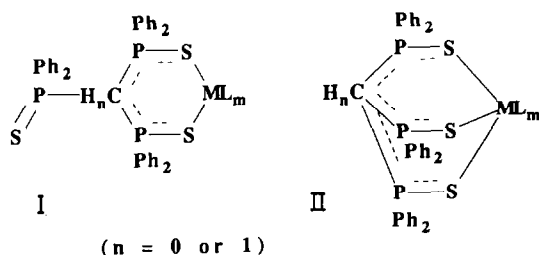
Abstract

Reactions of $[\text{MCl}(\text{cod})_2]$, $\text{M} = \text{Rh}$ or Ir , $\text{cod} = \text{cyclooctadiene}$, with $\text{CH}\{\text{P}(\text{S})\text{Ph}_2\}_3$ give the complex cations, $[\text{M}(\text{cod})\{\text{CH}(\text{P}(\text{S})\text{Ph}_2)_3\}]^+$, which are isolated in high yield as BF_4^- or ClO_4^- salts. These are the first reported examples of $\text{CH}\{\text{P}(\text{S})\text{Ph}_2\}_3$ complexes in which the methine proton is retained after coordination. The high acidity of this proton is demonstrated by easy deprotonation to corresponding $[\text{M}(\text{cod})\{\text{C}(\text{P}(\text{S})\text{Ph}_2)_3\}]$ complexes. The ^{31}P NMR spectrum of $[\text{Rh}(\text{cod})\{\text{CH}(\text{P}(\text{S})\text{Ph}_2)_3\}]\text{BF}_4$ remains a single line to -100°C whereas that of $[\text{Rh}(\text{cod})\{\text{C}(\text{P}(\text{S})\text{Ph}_2)_3\}]$ is resolved into two resonances at -60°C , suggesting that the former complex is 5-coordinate with an η^3 (S,S,S) ligand and the latter 4-coordinate, η^2 (S,S). The 4-coordinate structure is confirmed by X-ray diffraction studies of $[\text{Rh}(\text{cod})\{\text{C}(\text{P}(\text{S})\text{Ph}_2)_3\}]$ and $[\text{Ir}(\text{CO})_2\{\text{C}(\text{P}(\text{S})\text{Ph}_2)_3\}]$ which both show approximately square planar metal centers, η^2 ligands with the third sulfur non-coordinated ("dangling"), and trigonal planar geometry at the central carbon of the tris(phosphinesulfide) ligand. $[\text{Rh}(\text{cod})\{\text{C}(\text{P}(\text{S})\text{Ph}_2)_3\}]$ and $[\text{Ir}(\text{CO})_2\{\text{C}(\text{P}(\text{S})\text{Ph}_2)_3\}]$ crystallize in the *Pbca* space group ($Z=8$) with respective unit cells: $a = 20.427(4)$ Å, $b = 16.931(2)$ Å, $c = 23.138(3)$ Å; and $a = 22.140(6)$ Å, $b = 22.317(5)$ Å, $c = 14.792(3)$ Å. Line shape analysis for a variable temperature ^{31}P NMR study of $[\text{Rh}(\text{cod})\{\text{C}(\text{P}(\text{S})\text{Ph}_2)_3\}]$ gives ΔG^\ddagger 46 ± 2 kJ mol⁻¹ for the dynamic exchange of coordinated and non-coordinated sulfur.

Introduction

Tris(diphenylphosphinothioyl)methane, $\text{CH}\{\text{P}(\text{S})\text{Ph}_2\}_3$, was first reported by Issleib and Abicht [1] in 1970. This ligand and its derived anion, $[\text{C}\{\text{P}(\text{S})\text{Ph}_2\}_3]^-$, are potentially either 2, 4, or 6-electron donors and the anion is particularly interesting as a second example of a very rare class, namely tripodal anionic ligands [2]. The only previous example is the tris(pyrazolyl)borate ion, $[\text{HB}(\text{pz})_3]^-$, which has a diverse and well studied coordination chemistry [3,4], in strong contrast to the

relatively few reported complexes of $[C\{P(S)Ph_2\}_3]^-$. It is also noteworthy that there are no known examples of the coordinated neutral ligand, $CH\{P(S)Ph_2\}_3$. Evidently, attachment of a metal to the sulfur sites renders the methine proton too acidic, and under most reaction conditions this proton is spontaneously lost. Grim and co-workers [5] have reported cadmium and mercury complexes of the type $[MCl\{C\{P(S)Ph_2\}_3\}]$, and also examples of $[M(PR_3)\{C\{P(S)Ph_2\}_3\}]$, $M = Ag$ or Au [6]. An X-ray diffraction study shows the related mercury complex, $[HgCl\{C\{P(S)Me_2\}_2\{P(S)Ph_2\}\}]$, to contain an η^3 ligand (compare structure II), coordinated through the three sulfur atoms [5]. By way of contrast, the platinum complex, $[PtCl(PEt_3)\{C\{P(S)Ph_2\}_3\}]$, contains an η^2 ligand (compare structure I), which exhibits dynamic exchange between the non-coordinated $P=S$ group and that coordinated *trans* to phosphorus [7]. Coordination of the anion, $[C\{P(S)Ph_2\}_3]^-$, through carbon has not been observed, although the corresponding bis(phosphine sulfide) ion, $[CH\{P(S)Ph_2\}_2]^-$ is η^2 (*C,S*) coordinated in $[PtCl(PEt_3)\{CH\{P(S)Ph_2\}_2\}]$ [8].



The iridium and rhodium chemistry of these ligands has not been studied. It should be especially interesting since several literature studies indicate that ligands of these types may be effective in promoting catalysis at metal centres. Thus, the P,O chelate complex, $[RhCl(CO)\{Ph_2PCH_2CH_2P(O)Ph_2\}]$, catalyzes carbonylation of methanol to acetic acid [9] and iridium complexes of $[C\{P(O)Ph_2\}_3]^-$ are under investigation as catalysts in alkyne hydrosilylation [10]. Other authors have suggested that lability of $M-S$ bonds may occasion unusual reactivity and catalysis [11,12]. The analogy with trispyrazolyl borates is especially intriguing in this context since $[Rh(CO)(C_2H_4)\{HB(pz)_3\}]$ is known to activate benzene $C-H$ bonds [13]. During this reaction the ligand changes from η^2 (cf. I) to η^3 coordination (cf. II) and $[Rh(CO)H(Ph)\{HB(pz)_3\}]$ is formed. In the hydrosilylation study also, an initially η^2 ligand in $[Ir(C_2H_4)_2\{C\{P(O)Ph_2\}_3\}]$ is postulated to become η^3 in $[Ir(C_2H_4)H(SiR_3)\{C\{P(O)Ph_2\}_3\}]$ [10]. A primary difference between the $[C\{P(S)Ph_2\}_3]^-$ and $[HB(pz)_3]^-$ ligands is likely to be the facility of this change in coordination number, since in the former it requires that an essentially sp^2 carbon become non-planar. This problem does not arise with the neutral ligand, $CH\{P(S)Ph_2\}_3$, and we suggest that η^2 (structure I, $n=0$) is more likely for $[C\{P(S)Ph_2\}_3]^-$ and η^3 (structure II, $n=1$) for $CH\{P(S)Ph_2\}_3$. In either case dynamic ligand processes may be important.

The present paper describes results of our preliminary studies involving iridium and rhodium complexes of these ligands. We report the first examples of the coordinated neutral ligand in the cations, $[M(cod)\{CH\{P(S)Ph_2\}_3\}]^+$, $M = Rh$ or Ir , together with corresponding deprotonated complexes, $[M(cod)\{C\{P(S)Ph_2\}_3\}]$. Variable temperature ^{31}P NMR studies of the two rhodium complexes suggest that

the deprotonated, neutral complexes have $\eta^2,4$ -coordinate, structures of type I, whereas the cations are probably $\eta^3,5$ -coordinate, structures of type II. The type I structures are confirmed by X-ray diffraction studies of $[\text{Rh}(\text{cod})\{\text{C}(\text{P}(\text{S})\text{Ph}_2)_3\}]$ and $[\text{Ir}(\text{CO})_2\{\text{C}(\text{P}(\text{S})\text{Ph}_2)_3\}]$.

Experimental

a. Synthesis and spectroscopic studies

Data relating to the characterization of the complexes are given in the tables, the Results section and in the preparative descriptions below. Microanalysis was by the Canadian Microanalytical Service, Vancouver, B.C., Canada. Infrared spectra were recorded in KBr disks from 4000 to 200 cm^{-1} with an accuracy $\pm 3 \text{ cm}^{-1}$ on a Perkin Elmer 457 grating spectrophotometer calibrated against polystyrene film.

^1H , ^{31}P , and ^{13}C NMR spectra were recorded at 250.1, 101.3, and 62.9 MHz respectively, using a Bruker WM250 Fourier transform spectrometer, except that the variable temperature ^{31}P spectra were obtained at 145.9 MHz using a Bruker AMX360 spectrometer. Solvents were CDCl_3 or CH_2Cl_2 (see Table 1) and for the latter a lock signal was derived from the deuterium resonance of a capillary insert containing C_6D_6 . For ^{31}P and ^{13}C spectra, protons were decoupled by broad band ("noise") irradiation. ^1H and ^{13}C chemical shifts were measured relative to external $\text{Si}(\text{CH}_3)_4$. ^{31}P chemical shifts were measured relative to external $\text{P}(\text{OMe})_3$ and are reported in parts per million relative to 85% H_3PO_4 using a conversion factor of +141 ppm. For all nuclei, positive chemical shifts are downfield of the reference. Lineshapes for the dynamic ^{31}P NMR spectra were calculated using the DNMR3 program of Kleier and Binsch [14].

Except as noted below, all operations were carried out under an atmosphere of dry nitrogen using standard Schlenk tube techniques. Solvents were dried by appropriate methods and distilled under nitrogen prior to use. Recrystallizations from solvent pairs were by dissolution of the complex in the first solvent (using about double the volume required for complete solution) followed by dropwise addition or layering of sufficient second solvent to cause turbidity at ambient temperature. $\text{CH}\{\text{P}(\text{S})\text{Ph}_2\}_3$ [15] and $[\text{MCl}(\text{cod})]_2$ ($\text{M} = \text{Ir}, \text{Rh}$) [16,17] were synthesised as previously described.

$[\text{Rh}(\text{cod})\{\text{CH}(\text{P}(\text{S})\text{Ph}_2)_3\}]\text{BF}_4$. $\text{CH}\{\text{P}(\text{S})\text{Ph}_2\}_3$ (0.26 g, 0.40 mmol) in acetone (20 mL) was added to a stirred solution of $[\text{RhCl}(\text{cod})]_2$ (0.10 g, 0.20 mmol) and NaBF_4 (0.045 g, 0.41 mmol) in acetone (20 mL). The solution immediately became cloudy and changed in colour from yellow to orange. After 1 h the solution was filtered to remove precipitated NaCl , the solvent was removed *in vacuo*, and the residue crystallized from CH_2Cl_2 and hexanes to yield $[\text{Rh}(\text{cod})\{\text{CH}(\text{P}(\text{S})\text{Ph}_2)_3\}]\text{BF}_4$ as orange crystals (0.28 g, 0.29 mmol). Anal. Found: C, 55.4; H, 4.44. Calc. for $\text{C}_{45}\text{H}_{43}\text{BF}_4\text{P}_3\text{RhS}_3$: C, 56.2; H, 4.50%.

$[\text{Ir}(\text{cod})\{\text{CH}(\text{P}(\text{S})\text{Ph}_2)_3\}]\text{ClO}_4$. This preparation was similar to that described above for the rhodium analog except that $\text{NaClO}_4 \cdot \text{H}_2\text{O}$ was used in place of NaBF_4 to yield $[\text{Ir}(\text{cod})\{\text{CH}(\text{P}(\text{S})\text{Ph}_2)_3\}]\text{ClO}_4$ as yellow crystals in 78% yield. Anal. Found: C, 51.0; H, 4.32. Calc. for $\text{C}_{45}\text{H}_{43}\text{ClIrO}_4\text{P}_3\text{S}_3$: C, 50.8; H, 4.07%.

$[\text{Rh}(\text{cod})\{\text{C}(\text{P}(\text{S})\text{Ph}_2)_3\}]$. Dichloromethane (10 mL) was added with stirring to a mixture of $\text{CH}\{\text{P}(\text{S})\text{Ph}_2\}_3$ (0.13 g, 0.20 mmol) and $[\text{RhCl}(\text{cod})]_2$ (0.048 g, 0.10 mmol) to give a yellow solution. After 5 min a few drops of diethylamine (ca. 0.2

mL) were added. The solvent was removed *in vacuo* and the residue extracted with toluene (10 mL). Solvent was removed from the extract *in vacuo* and the residue recrystallized from dichloromethane and hexanes to yield $[\text{Rh}(\text{cod})\{\text{C}(\text{P}(\text{S})\text{Ph}_2)_3\}]$ as yellow crystals (0.12 g, 0.14 mmol). Anal. Found: C, 61.5; H, 4.86. Calc. for $\text{C}_{45}\text{H}_{42}\text{RhP}_3\text{S}_3$: C, 61.8; H, 4.84%.

$[\text{Ir}(\text{cod})\{\text{C}(\text{P}(\text{S})\text{Ph}_2)_3\}]$. This preparation was similar to that described above for the rhodium analog and gave $[\text{Ir}(\text{cod})\{\text{C}(\text{P}(\text{S})\text{Ph}_2)_3\}]$ as yellow crystals in 66% yield. Anal. Found: C, 55.9; H, 4.55. Calc. for $\text{C}_{45}\text{H}_{42}\text{IrP}_3\text{S}_3$: C, 56.1; H, 4.39%.

$[\text{Ir}(\text{CO})_2\{\text{C}(\text{P}(\text{S})\text{Ph}_2)_3\}]$. Carbon monoxide was bubbled for about 1 min though a solution of $[\text{Ir}(\text{cod})\{\text{C}(\text{P}(\text{S})\text{Ph}_2)_3\}]$ (0.10 g, 0.10 mmol) in toluene (25 mL), resulting in a rapid lessening of the yellow colour. Solvent was removed *in vacuo*, and the residue was washed with hexanes (3×5 mL) and recrystallised from dichloromethane/hexanes to give $[\text{Ir}(\text{CO})_2\{\text{C}(\text{P}(\text{S})\text{Ph}_2)_3\}]$ as pale yellow crystals (0.060 g, 0.066 mmol). Anal. Found: C, 51.0; H, 3.33. Calc. for $\text{C}_{39}\text{H}_{30}\text{IrO}_2\text{P}_3\text{S}_3$: C, 51.4; H, 3.32%. Infrared: 2040(s), 1965(s,br) cm^{-1} .

b. X-Ray data collection

$[\text{Rh}(\text{cod})\{\text{C}(\text{P}(\text{S})\text{Ph}_2)_3\}]$ and $[\text{Ir}(\text{CO})_2\{\text{C}(\text{P}(\text{S})\text{Ph}_2)_3\}]$ were prepared as described above and crystals suitable for study by X-ray diffraction were grown by recrystallization from dichloromethane/hexanes. Preliminary photographic work was carried out with Weissenberg and precession cameras using $\text{Cu-K}\alpha$ radiation. After establishment of symmetry and approximate unit cells the crystals were transferred to a Picker 4-circle diffractometer automated with a PDP11/10 computer and the unit cells refined by least squares methods employing pairs of centering measurements (see Table 2). Diffraction data were collected using a $\theta/2\theta$ step scan with 160 steps of 0.01° in 2θ , counting for 0.25 s per step. Background measurements were for 20 s at each end of the scan. Each batch of 50 reflections was preceded by the measurement of three standard reflections, and, after application of Lorentz and polarization factors, each batch was scaled to maintain the sum of the standards constant. Absorption corrections were applied by a numerical integration using a Gaussian grid and with the crystal shape defined by perpendicular distances to crystal faces from a central origin. There was no evidence of decomposition during data collection for either crystal.

c. Structure solution and refinement

The structures were found and refined using the SHELX-76 program package [18], and illustrations were drawn using ORTEP [19]. The atomic scattering factors used were for neutral atoms, with corrections for anomalous dispersion [20]. The structures were solved by direct methods, developed by standard Fourier synthesis procedures using difference maps, and refined by the method of least squares minimising $\Sigma w\Delta^2$ where $\Delta = \|F_o| - |F_c\|$. The weights were obtained from counting statistics using $w = 1/(\sigma^2(F) + 0.001F^2)$. The metal atoms, all phosphorus and sulfur atoms, the central carbons of the $\text{C}(\text{P}(\text{S})\text{Ph}_2)_3$ ligands, and the carbons of the cod ligand were treated anisotropically; the remaining carbon atoms isotropically. Hydrogen atoms were not located. The final difference maps for I showed small peaks (ca. $1.6 \text{ e } \text{\AA}^{-3}$) near the iridium atoms but neither structure gave any indication that material had been overlooked.

Results and discussion

a. Synthesis

Reactions of $[MCl(cod)]_2$ ($M = Rh, Ir, cod = cyclooctadiene$) with two molar equivalents of $CH\{P(S)Ph_2\}_3$, in acetone in the presence of BF_4^- or ClO_4^- , result in cleavage of the chloro-bridges and formation of $[M(cod)\{CH\{P(S)Ph_2\}_3\}][Z]$ in high yield. These are the first complexes reported of $CH\{P(S)Ph_2\}_3$ in which the methine proton remains intact on the ligand after coordination to the metal centre. However, the high acidity of this proton is still evident from corresponding reactions in dichloromethane with added base (diethylamine), which result in deprotonated neutral complexes, $[M(cod)\{C(P(S)Ph_2)_3\}]$. Reaction of carbon monoxide with $[Ir(cod)\{C(P(S)Ph_2)_3\}]$ produces $[Ir(CO)_2\{C(P(S)Ph_2)_3\}]$ in high yield.

b. Ambient temperature NMR spectra

Nuclear magnetic resonance parameters for the complexes are collected in Table 1. The 1H spectra serve mainly to confirm the presence of the methine proton in the cationic complexes. These resonances appear as quartets with typical two bond P–H couplings of about 11 Hz, and the interpretation is also confirmed by multiplicity sorting (DEPT) experiments on the ^{13}C spectra. The ^{31}P spectra all show essentially single resonances at ambient temperature, although for $[Rh(cod)\{C(P(S)Ph_2)_3\}]$ there is evidence of a small doublet coupling to rhodium (3 Hz). The shift range is extremely narrow (+37.2 to +41.4 ppm) illustrating the insensitivity of the phosphorus nuclei to the nature of the metal, the charge on the complex, and the type of other ligands attached. The shifts are similar to those observed in platinum [7], cadmium and mercury [5] complexes, and the neutral ligand complexes in particular show only very small coordination shifts from the free ligand (Table 1). Shifts from the free to coordinated anion are larger, with increased shielding of about 5–8 ppm.

Two different coordination modes can be postulated for the tris(phosphine sulfide) ligands in these complexes, a bidentate mode, I, and a tridentate mode, II. It is evident that a static structure I would give at least two different phosphorus

Table 1

Selected nuclear magnetic resonance parameters for complexes of $C_AH_A(P(S)Ph_2)_3$ and $[C_A(P(S)Ph_2)_3]^-$

Complex	Notes	$\delta(P)$	$\delta(C_A)$	$J(P-C_A)$	$\delta(H_A)$	$J(P-H_A)$
$[Rh(cod)\{CH\{P(S)Ph_2\}_3\}]^+$	<i>ac</i>	41.4	35.3	29	6.18	11
$[Ir(cod)\{CH\{P(S)Ph_2\}_3\}]^+$	<i>bc</i>	41.2	31.2	38	6.28	11
$[Rh(cod)\{C(P(S)Ph_2)_3\}]$	<i>de</i>	39.8	<i>f</i>	<i>f</i>	–	–
$[Ir(cod)\{C(P(S)Ph_2)_3\}]$	<i>d</i>	37.2	<i>f</i>	<i>f</i>	–	–
$[Ir(CO)_2\{C(P(S)Ph_2)_3\}]$	<i>c</i>	37.7	<i>f</i>	<i>f</i>	–	–
$CH\{P(S)Ph_2\}_3$	<i>cg</i>	41.9	52.1	22	6.04	17
$[C(P(S)Ph_2)_3]^-$	<i>cgh</i>	45.2	33.1	76	–	–

Chemical shifts (δ) are quoted in parts per million relative to $Si(CH_3)_4$ for 1H and ^{13}C and 85% H_3PO_4 for ^{31}P . All shifts are positive. Coupling constants (J) are in Hertz.

^a BF_4^- salt. ^b ClO_4^- salt. ^c $CDCl_3$ solution. ^d CH_2Cl_2 solution with external C_6D_6 lock. ^e Variable temperature spectra in tetrahydrofuran-*d*₈ solution show two shifts, 41.8 and 38.8 ppm, in a 1:2 ratio at $-70^\circ C$ and a single shift, 40.1 ppm, at magnet ambient ($+26^\circ C$). ^f Not observed due to low solubility and high multiplicity. ^g Data from ref. 2. ^h Li^+ salt.

environments and possibly three if the other ligands, L_m , were asymmetric. Moreover, if L_m consists of a bidentate ligand, or two monodentate ligands, as in the present complexes, then two different environments are also expected for the phosphorus atoms of structure II. In either case a dynamic intramolecular exchange process could produce the single line phosphorus spectra reported above and a low temperature study is needed (see below). However, since the overall range of chemical shifts from complex to complex is very narrow, we may expect that the differences within structure II would be very small indeed and not easily resolved even at low temperature.

c. Variable temperature ^{31}P NMR

The ^{31}P NMR spectrum of $[\text{Rh}(\text{cod})\{\text{H}(\text{P}(\text{S})\text{Ph}_2)_3\}]\text{BF}_4$ remains a sharp single line, width about 15 Hz, from ambient temperature down to -100°C , suggesting either a very facile exchange process or very small chemical shift differences, or both. Whichever is correct, it seems likely that this complex has a tridentate structure of type II. In contrast, the low temperature ^{31}P NMR spectrum of $[\text{Rh}(\text{cod})\{\text{C}(\text{P}(\text{S})\text{Ph}_2)_3\}]$ shows a clear resolution into two peaks. The spectra over the temperature range from ambient to -60°C are shown in Fig. 1, together with line shape simulations derived from the DNMR3 computer program of Kleier and Binsch [14]. The simulations assume an exchange process based on an η^2 structure of type I, with two different chemical shifts in a 2:1 ratio at the slow exchange limit and with complete mutual exchange at the fast exchange limit. Spectra at lower temperatures show broadening of the high field (intensity 2) resonance, probably due to non-equivalence of the two coordinated $\text{P}(\text{S})\text{Ph}_2$ groups caused by restricted rotation of the "dangling" $\text{P}(\text{S})\text{Ph}_2$ group, but we have not yet obtained spectra at low enough temperatures to completely characterize this second process. Rate constants obtained from line shape fitting for the exchange process over the -54 to $+26^\circ\text{C}$ range (Fig. 1) vary from 10 to $40,000\text{ s}^{-1}$, and at the coalescence temperature of -44°C the rate is 425 s^{-1} . An Eyring plot of $\ln(k_r/T)$ against $1/T$ gives a good straight line and activation parameters as follows: $\Delta H^{\ddagger} 38 \pm 2\text{ kJ mol}^{-1}$; $\Delta S^{\ddagger} -27 \pm 3\text{ J K}^{-1}$; $\Delta G^{\ddagger} 46 \pm 2\text{ kJ mol}^{-1}$.

It is interesting to compare these data with the significantly higher activation barriers found previously [7] in platinum complexes of $[\text{C}\{\text{P}(\text{S})\text{Ph}_2\}_3]^-$. For $[\text{PtCl}(\text{PEt}_3)\{\text{C}(\text{P}(\text{S})\text{Ph}_2)_3\}]$ the barrier is 67.1 kJ mol^{-1} and the dynamic process involves a pivotal motion about the relatively strong Pt-S bond *trans* to Cl. Only the relatively weakly bound P=S group *trans* to PEt_3 is involved in exchange with the non-coordinated P=S group. The process in $[\text{Pt}(\text{PEt}_3)_2\{\text{C}(\text{P}(\text{S})\text{Ph}_2)_3\}]^+$, $\Delta G^{\ddagger} 61.3\text{ kJ mol}^{-1}$, is more closely comparable to the present rhodium example with exchange of all three phosphorus environments. The significance of the lower barriers in the rhodium complex is emphasized by the fact that the two different mechanisms in the platinum complexes produce only a small difference in activation parameters. Thus, in the rhodium complex the transition state, presumably 5-coordinate, is significantly stabilized relative to those in the platinum examples, and this is consistent with our suggestion that in the $[\text{M}(\text{cod})\{\text{CH}(\text{P}(\text{S})\text{Ph}_2)_3\}]^+$ cations, the ground-state structure is 5-coordinate.

d. X-Ray structures of $[\text{Rh}(\text{cod})\{\text{C}(\text{P}(\text{S})\text{Ph}_2)_3\}]$ and $[\text{Ir}(\text{CO})_2\{\text{C}(\text{P}(\text{S})\text{Ph}_2)_3\}]$

These structures are shown as ORTEP diagrams in Figs. 2 and 3 respectively. Unit cell and other parameters related to the crystal structure determinations are in Table

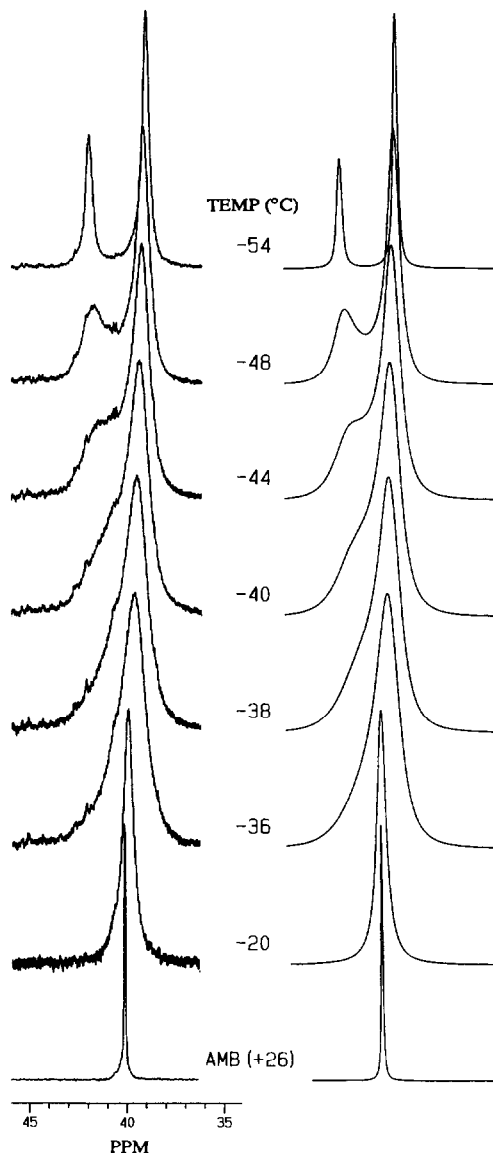


Fig. 1. Observed and calculated line shapes for the ^{31}P NMR spectrum of $[\text{Rh}(\text{cod})\{\text{C}(\text{P}(\text{S})\text{Ph}_2)_3\}]$.

2, selected fractional atomic coordinates in Tables 3 and 4, selected bond lengths in Table 5, and selected bond angles in Table 6 [21*].

Both structures consist of approximately square planar metal centers with $[\text{C}(\text{P}(\text{S})\text{Ph}_2)_3]^-$ anions coordinated in a bidentate fashion through two sulfur atoms, and with the third sulfur non-coordinated (“dangling”). There are relatively small distortions of the square planes, for example in the iridium complex, the carbonyl

* Reference number with asterisk indicates a note in the list of references.

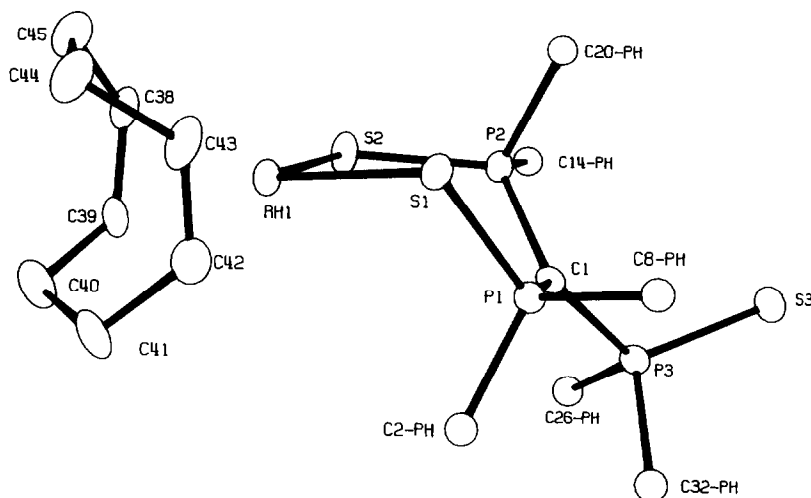


Fig. 2. ORTEP plot for a single molecule of $[\text{Rh}(\text{cod})\{\text{C}(\text{P}(\text{S})\text{Ph}_2)_3\}]$.

carbons, C(2) and C(3), are respectively $+0.286$ and -0.109 Å from the plane defined by Ir–S(1)–S(2). Angles at the metal centers are close to 90° , ranging from 86.7 to 93.4° , but in both complexes the largest angle is subtended by the chelate ligand, S(1)–M–S(2) 93.4° , M = Rh or Ir. This was also true in the platinum complex, $[\text{PtCl}(\text{PET}_3)\{\text{C}(\text{P}(\text{S})\text{Ph}_2)_3\}]$ (S–Pt–S 94.9°), reported previously [7] and suggests that a bite angle slightly greater than 90° is a necessary requirement for this ligand. The metal sulfur lengths, av. 2.35 (Rh), 2.36 Å (Ir), are relatively long but in the same range as observed previously in related platinum complexes. In $[\text{PtCl}(\text{PET}_3)\{\text{C}(\text{P}(\text{S})\text{Ph}_2)_3\}]$ the Pt–S lengths are 2.28 and 2.35 Å, *trans* to C1 and

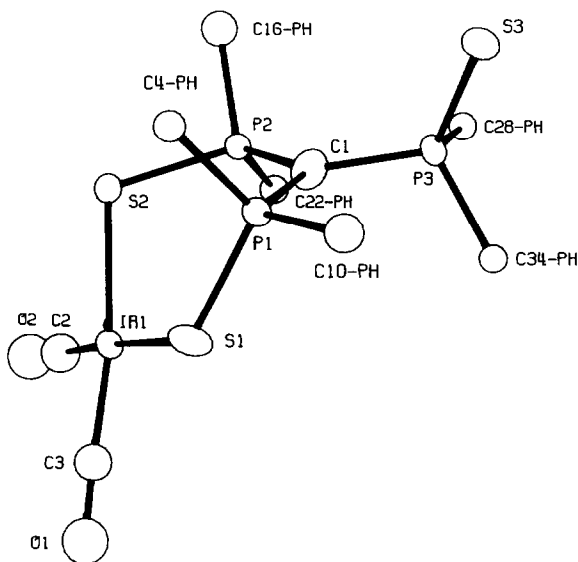


Fig. 3. ORTEP plot for a single molecule of $[\text{Ir}(\text{CO})_2\{\text{C}(\text{P}(\text{S})\text{Ph}_2)_3\}]$.

Table 2
Selected crystallographic data

	[Rh(cod){C(P(S)Ph ₂) ₃ }]	[Ir(CO) ₂ {C(P(S)Ph ₂) ₃ }]
Formula	C ₄₅ H ₄₂ P ₃ RhS ₃	C ₃₉ H ₃₀ IrO ₂ P ₃ S ₃
fw	874.8	912.0
Space group	<i>Pbca</i> (No. 61)	<i>Pbca</i> (No. 61)
<i>a</i> , Å	20.427(4)	22.140(6)
<i>b</i> , Å	16.931(2)	22.317(5)
<i>c</i> , Å	23.138(3)	14.792(3)
<i>V</i> , Å ³	8002	7309
<i>Z</i>	8	8
Density, calc/obs, g cm ⁻³	1.43/1.46	1.66/1.64
Diffraction	Picker 4-circle	Picker 4-circle
Radiation (λ, Å)	Mo-K _α (0.71069)	Mo-K _α (0.71069)
μ, cm ⁻¹	7.19	42.06
Transmission factor range	0.86–0.91	0.45–0.73
Temperature, K	295	295
No. of observed reflections (<i>I</i> > 2σ(<i>I</i>))	3400	1994
<i>R</i>	0.067	0.068
<i>R_w</i>	0.067	0.068

$$R = (\Sigma \Delta / \Sigma F_o); R_w = (\Sigma w \Delta^2 / \Sigma w F_o^2)^{1/2}; w = 1/(\sigma^2(F) + 0.001F^2); \Delta = \| F_o \| - | F_c |.$$

Table 3
Selected fractional atomic coordinates and temperature parameters for [Rh(cod){C(P(S)Ph₂)₃}]

Atom	<i>x</i>	<i>y</i>	<i>z</i>	<i>U_{eq}</i>
Rh(1)	7777(4)	6349(5)	-32768(3)	318(3)
S(1)	1556(1)	466(2)	-2535(1)	34(1)
S(2)	-112(1)	490(2)	-2650(1)	41(1)
S(3)	502(2)	1447(2)	-237(1)	41(1)
P(1)	1447(1)	1348(2)	-1951(1)	29(1)
P(2)	186(1)	506(2)	-1809(1)	29(1)
P(3)	460(1)	1927(2)	-1011(1)	31(1)
C(1)	669(5)	1311(6)	-1605(4)	29(4)
C(2)	1587(5)	2293(6)	-2314(4)	32(3)'
C(8)	2165(5)	1195(6)	-1488(4)	32(3)'
C(14)	-588(5)	508(6)	-1416(4)	32(3)'
C(20)	556(5)	-430(6)	-1597(4)	29(3)'
C(26)	-365(5)	2339(6)	-1137(4)	34(3)'
C(32)	1001(5)	2795(6)	-1046(5)	35(3)'
C(38)	157(6)	220(8)	-3971(5)	42(5)
C(39)	161(6)	1048(8)	-3983(5)	45(5)
C(40)	526(7)	1532(8)	-4437(5)	59(5)
C(41)	1219(7)	1773(8)	-4222(5)	63(6)
C(42)	1513(6)	1187(8)	-3792(5)	48(5)
C(43)	1539(6)	358(8)	-3877(5)	52(5)
C(44)	1280(6)	-47(8)	-4423(5)	58(5)
C(45)	565(7)	-317(8)	-4339(5)	60(5)

Estimated standard deviations are given in parentheses. Coordinates $\times 10^n$ where $n = 5$ for Rh and 4 otherwise. Temperature parameters $\times 10^n$ where $n = 4$ for Rh and 3 otherwise. U_{eq} is the equivalent isotropic temperature parameter: $U_{eq} = 1/3 \Sigma_i \Sigma_j U_{ij} a_i^* a_j^* (a_i \cdot a_j)$. Primed values indicate that U_{iso} is given. $T = \exp(-8\pi^2 U_{iso} \sin^2 \theta / \lambda^2)$.

Table 4

Selected fractional atomic coordinates and temperature parameters for $[\text{Ir}(\text{CO})_2\{\text{C}(\text{P}(\text{S})\text{Ph}_2)_3\}]$

Atom	<i>x</i>	<i>y</i>	<i>z</i>	U_{eq}
Ir(1)	37404(6)	7316(5)	21581(7)	434(4)
S(1)	4456(4)	44(4)	2700(6)	58(3)
S(2)	3298(4)	27(3)	1158(5)	41(3)
S(3)	3509(4)	-2390(3)	3062(5)	57(3)
P(1)	4198(4)	-825(4)	2409(5)	35(3)
P(2)	2914(3)	-644(3)	1907(4)	35(3)
P(3)	3250(4)	-1577(3)	3402(5)	40(3)
O(1)	4424(12)	1666(12)	3202(17)	96(8)'
O(2)	2795(13)	1611(13)	1617(18)	104(9)'
C(1)	3437(15)	-1005(14)	2578(19)	54(13)
C(2)	3187(16)	1260(16)	1839(23)	74(11)'
C(3)	4156(15)	1300(15)	2775(23)	64(9)'
C(4)	4442(12)	-997(12)	1265(18)	40(8)'
C(10)	4711(14)	-1251(14)	3115(21)	60(10)'
C(16)	2583(15)	-1107(15)	1008(21)	59(9)'
C(22)	2262(12)	-339(12)	2500(16)	38(8)'
C(28)	2436(12)	-1597(11)	3557(17)	35(7)'
C(34)	3540(11)	-1347(11)	4499(17)	33(7)'

Estimated standard deviations are given in parentheses. Coordinates $\times 10^n$ where $n = 5$ for Ir and 4 otherwise. Temperature parameters $\times 10^n$ where $n = 4$ for Ir and 3 otherwise. U_{eq} = the equivalent isotropic temperature parameter: $U_{\text{eq}} = 1/3 \sum_i \sum_j U_{ij} a_i^* a_j^* (a_i \cdot a_j)$. Primed values indicate that U_{iso} is given. $T = \exp(-8\pi^2 U_{\text{iso}} \sin^2 \theta / \lambda^2)$.

PEt_3 respectively [7], and in the related bis(phosphine chalcogenide) complex, $[\text{PtCl}(\text{PEt}_3)\{\text{CH}(\text{P}(\text{S})\text{Ph}_2)_2\}]$, the Pt-S length is 2.39 Å *trans* to PEt_3 [8].

In both complexes the metals and the chelate ligands form 6-membered rings in

Table 5

Selected interatomic distances (Å)

$[\text{Rh}(\text{cod})\{\text{C}(\text{P}(\text{S})\text{Ph}_2)_3\}]$		$[\text{Ir}(\text{CO})_2\{\text{C}(\text{P}(\text{S})\text{Ph}_2)_3\}]$	
S(1)-Rh(1)	2.356(3)	S(1)-Ir(1)	2.348(8)
S(2)-Rh(1)	2.337(3)	S(2)-Ir(1)	2.370(7)
C(38)-Rh(1)	2.163(10)	C(3)-Ir(1)	1.81(3)
C(39)-Rh(1)	2.178(11)	C(2)-Ir(1)	1.77(4)
C(42)-Rh(1)	2.133(11)	P(1)-S(1)	2.066(11)
C(43)-Rh(1)	2.137(11)	P(2)-S(2)	2.048(10)
P(1)-S(1)	2.027(4)	P(3)-S(3)	1.969(10)
P(2)-S(2)	2.039(4)	C(1)-P(1)	1.76(3)
P(3)-S(3)	1.968(4)	C(4)-P(1)	1.82(3)
C(1)-P(1)	1.781(10)	C(10)-P(1)	1.81(3)
C(2)-P(1)	1.829(10)	C(1)-P(2)	1.73(3)
C(8)-P(1)	1.834(10)	C(16)-P(2)	1.84(3)
C(1)-P(2)	1.749(10)	C(22)-P(2)	1.82(3)
C(14)-P(2)	1.824(10)	C(1)-P(3)	1.81(3)
C(20)-P(2)	1.824(10)	C(28)-P(3)	1.82(3)
C(1)-P(3)	1.776(10)	C(34)-P(3)	1.82(3)
C(26)-P(3)	1.848(11)	C(2)-O(2)	1.22(4)
C(32)-P(3)	1.841(11)	C(3)-O(1)	1.19(4)

Estimated standard deviations are given in parentheses.

Table 6

Selected bond angles ($^{\circ}$)

[Rh(cod){C(P(S)Ph ₂) ₃ }]		[Ir(CO) ₂ {C(P(S)Ph ₂) ₃ }]	
S(2)–Rh(1)–S(1)	93.4(1)	S(2)–Ir(1)–S(1)	93.4(3)
C(38)–Rh(1)–S(2)	153.7(4)	C(3)–Ir(1)–S(1)	86.7(10)
C(38)–Rh(1)–S(2)	88.3(3)	C(3)–Ir(1)–S(2)	170.9(11)
C(39)–Rh(1)–S(1)	167.2(3)	C(2)–Ir(1)–S(1)	175.5(11)
C(39)–Rh(1)–S(2)	92.8(3)	C(2)–Ir(1)–S(2)	89.4(11)
C(39)–Rh(1)–C(38)	37.7(4)	C(2)–Ir(1)–C(3)	91.2(15)
C(42)–Rh(1)–S(1)	89.2(3)	P(1)–S(1)–Ir(1)	110.8(4)
C(42)–Rh(1)–S(2)	160.0(4)	P(2)–S(2)–Ir(1)	108.6(4)
C(42)–Rh(1)–C(38)	98.0(5)	C(1)–P(1)–S(1)	116.9(11)
C(42)–Rh(1)–C(39)	81.2(5)	C(4)–P(1)–S(1)	108.0(10)
C(43)–Rh(1)–S(1)	87.4(3)	C(4)–P(1)–C(1)	111.8(4)
C(43)–Rh(1)–S(2)	161.1(4)	C(10)–P(1)–S(1)	101.5(11)
P(43)–Rh(1)–C(38)	82.7(5)	C(10)–P(1)–C(1)	113.6(14)
C(43)–Rh(1)–C(39)	90.3(5)	C(10)–P(1)–C(4)	103.9(14)
C(43)–Rh(1)–C(42)	38.8(4)	C(1)–P(2)–S(2)	112.0(12)
P(1)–S(1)–Rh(1)	108.8(1)	C(16)–P(2)–S(2)	100.7(11)
P(2)–S(2)–Rh(1)	111.0(1)	C(16)–P(2)–C(1)	114.9(15)
C(1)–P(1)–S(1)	111.8(4)	C(22)–P(2)–S(2)	108.5(9)
C(2)–P(1)–S(1)	108.7(3)	C(22)–P(2)–C(1)	115.4(13)
C(2)–P(1)–C(1)	112.1(5)	C(22)–P(2)–C(16)	104.1(14)
C(8)–P(1)–S(1)	101.5(4)	C(1)–P(3)–S(3)	114.2(10)
C(8)–P(1)–C(1)	116.5(5)	C(28)–P(3)–S(3)	107.4(9)
C(8)–P(1)–C(2)	105.4(5)	C(28)–P(3)–C(1)	109.2(13)
C(1)–P(2)–S(2)	115.9(4)	C(34)–P(3)–S(3)	112.6(9)
C(14)–P(2)–S(2)	102.6(4)	C(34)–P(3)–C(1)	108.7(13)
C(14)–P(2)–C(1)	110.6(5)	C(34)–P(3)–C(28)	104.2(12)
C(20)–P(2)–S(2)	111.7(3)	O(1)–C(3)–Ir(1)	178 (3)
C(20)–P(2)–C(1)	111.8(5)	O(2)–C(2)–Ir(1)	178 (3)
C(20)–P(2)–C(14)	103.1(5)	P(2)–C(1)–P(1)	117 (2)
C(1)–P(3)–S(3)	116.8(3)	P(3)–C(1)–P(1)	119 (2)
C(26)–P(3)–S(3)	109.8(4)	P(3)–C(1)–P(2)	124 (2)
C(26)–P(3)–C(1)	108.6(5)		
C(32)–P(3)–S(3)	110.0(4)		
C(32)–P(3)–C(1)	106.9(5)		
C(32)–P(3)–C(26)	103.9(5)		
P(2)–C(1)–P(1)	114.2(5)		
P(3)–C(1)–P(1)	122.8(6)		
P(3)–C(1)–P(2)	122.1(6)		
C(39)–C(38)–Rh(1)	71.7(7)		
C(38)–C(39)–Rh(1)	70.6(7)		
C(43)–C(42)–Rh(1)	70.8(7)		
C(42)–C(43)–Rh(1)	70.4(7)		

Estimated standard deviations are given in parentheses.

approximate boat conformations with sulfur and phosphorus at the prows and with the M–S bond forming one side of the boat. Within the ring, the angles at sulfur are close to tetrahedral, 108–111 $^{\circ}$, and those at phosphorus slightly larger, 112–117 $^{\circ}$. These angles at phosphorus are very similar to those in the non-coordinated PS group, C(1)–P(3)–S(3) 117 (Rh) and 114 $^{\circ}$ (Ir), indicating that hybridization at phosphorus is not significantly affected by coordination of the sulfur. As expected,

the P–S bonds to coordinated sulfur, 2.03–2.07 Å, are slightly longer than those to the non-coordinated sulfur, 1.97 Å. These lengths may be compared with those in $[\text{N}^n\text{Bu}_4][\text{C}\{\text{P}(\text{S})\text{Ph}_2\}_3]$, av. 1.976 Å [22], and $\text{CH}\{\text{P}(\text{S})\text{Ph}_2\}_3$, av. 1.944 Å [23].

The most important structural observation is the closely planar arrangement of phosphorus atoms around C(1). P(3) is 0.28 Å from the P(1)–C(1)–P(2) plane in the rhodium structure and 0.073 Å for iridium. The trigonal planar geometry at C(1) is also evident in the P–C–P angles, 114–122° (Rh) and 117–124° (Ir), and is clear confirmation of deprotonation of the ligand. The P–C bonds, 1.72–1.81 Å, are similar in length to those in $[\text{N}^n\text{Bu}_4][\text{C}\{\text{P}(\text{S})\text{Ph}_2\}_3]$, av. 1.76 Å [22], shorter than in $\text{CH}\{\text{P}(\text{S})\text{Ph}_2\}_3$, av. 1.88 Å [23], and considerably longer than those in typical ylides, 1.62–1.66 Å [24,25]. These comparisons clearly show the delocalized, partially double bonded structure of the coordinated anions.

Acknowledgements

We thank the Natural Sciences and Engineering Research Council of Canada and the University of Victoria for research grants, Mrs K. Beveridge for technical assistance in the crystal structure determinations, and Mrs C. Greenwood for recording NMR spectra.

References and notes

- 1 K. Issleib and H.P. Abicht, *J. Prakt. Chem.*, 312 (1970) 456.
- 2 S.O. Grim, S.A. Sangokoya, I.J. Colquhoun, W. McFarlane and R.K. Khanna, *Inorg. Chem.*, 25 (1986) 2699.
- 3 S. Trofimenko, *Acc. Chem. Res.*, 4 (1971) 17.
- 4 S. Trofimenko, *Chem. Rev.*, 72 (1972) 497.
- 5 S.O. Grim, P.H. Smith, S. Nittolo, H.L. Ammon, L.C. Satek, S.A. Sangokoya, R.K. Khanna, I.J. Colquhoun, W. McFarlane and J.R. Holden, *Inorg. Chem.*, 24 (1985) 2889.
- 6 S.O. Grim, S.A. Sangokoya, R.D. Gilardi, I.J. Colquhoun and W. McFarlane, paper presented at the 23rd International Conference on Coordination Chemistry, Boulder, CO, 1984.
- 7 J. Browning, K.A. Beveridge, G.W. Bushnell and K.R. Dixon, *Inorg. Chem.*, 25 (1986) 1987.
- 8 J. Browning, G.W. Bushnell, K.R. Dixon and A. Pidcock, *Inorg. Chem.*, 22 (1983) 2226.
- 9 R.W. Wegman, A.G. Abatjoglou and A.M. Harrison, *J. Chem. Soc., Chem. Commun.*, (1987) 1891.
- 10 R.S. Tanke and R.H. Crabtree, *J. Chem. Soc., Chem. Commun.*, (1990) 1056.
- 11 A.M. Mazany and J.P. Fackler, *Organometallics*, 1 (1982) 752.
- 12 B.R. James and F.T.T. Ng, *J. Chem. Soc., Dalton Trans.*, (1972) 355.
- 13 C.K. Ghosh, D.P.S. Rodgers and W.A.G. Graham, *J. Chem. Soc., Chem. Commun.*, (1988) 1511.
- 14 D.A. Kleier and G. Binsch, Quantum Chemistry Program Exchange, Program No. 165, University of Indiana, Bloomington, IN, 1969.
- 15 S.O. Grim, L.C. Satek and J.D. Mitchell, *Z. Naturforsch. B., Anorg. Chem. Org. Chem.*, B35 (1980) 832.
- 16 J.L. Herde, J.C. Lambert and C.V. Senoff, *Inorg. Synth.*, 15 (1974) 18.
- 17 G. Giordano and R.H. Crabtree, *Inorg. Synth.*, 19 (1979) 218.
- 18 G.M. Sheldrick, *SHELX-76*, A computer Program for Crystal Structure Determination, University of Cambridge, England, (1976).
- 19 C.K. Johnson, *ORTEP*, Report ORNL-3794, Oak Ridge National Laboratory, Oak Ridge, TN, 1965.
- 20 D.T. Cromer and J.T. Waber, in J.A. Ibers and W.C. Hamilton (Eds.), *International Tables for X-ray Crystallography*, Vol. IV, Kynoch Press, Birmingham, England, 1974.
- 21 Supplementary material available from the authors: For $[\text{Rh}(\text{cod})\{\text{C}(\text{P}(\text{S})\text{Ph}_2)_3\}]$ and $[\text{Ir}(\text{CO})_2\{\text{C}(\text{P}(\text{S})\text{Ph}_2)_3\}]$: unit cell, data collection and refinement parameters (Table S1), fractional atomic coordinates and isotropic temperature parameters for all atoms (Tables S2, S3), anisotropic temperature factors for the heavy atoms (Tables S4, S5), interatomic distances (Tables S6, S7), bond angles

- (Tables S8, S9), selected intermolecular distances (Tables S10, S11) (14 pages); observed and calculated structure factor amplitudes (Tables S12, S13) (24 pages).
- 22 S.O. Grim, R.D. Gilardi and S.A. Sangokoya, *Angew. Chem., Int. Ed. Engl.*, 22 (1983) 254.
 - 23 I.J. Colquhoun, W. McFarlane, J.M. Bassett and S.O. Grim, *J. Chem. Soc., Dalton Trans.*, (1981) 1645.
 - 24 J.C.J. Bart, *J. Chem. Soc. B*, (1969) 350.
 - 25 H. Schmidbaur, V. Deschler and B. Nilewski-Mahla, *Chem. Ber.*, 116 (1981) 1393.